Published in final edited form as:
Nat Struct Mol Biol. 2008 April ; 15(4): 403–410. doi:10.1038/nsmb.1398.

Reciprocal regulation of the Ca^{2+} and H^+ sensitivity in the Slo1 BK channel conferred by the RCK1 domain

Shangwei Hou[1], **Rong Xu**[1], **Stefan H. Heinemann**[2], and **Toshinori Hoshi**[1]

[1] Department of Physiology, University of Pennsylvania, Philadelphia, 3700 Hamilton Walk, Philadelphia, Pennsylvania 19104, USA

[2] Center for Molecular Biomedicine, Department of Biophysics, Friedrich Schiller University Jena, Hans-Knöll-St. 2, D-07745 Jena, Germany

Abstract

Increasing evidence suggests that intracellular H^+ directly stimulates large-conductance Ca^{2+}- and voltage-activated K^+ (Slo1 BK) channels, thus providing a crucial link between membrane excitability and cell metabolism. Here we report that two histidine residues, His365 and His394, located in the intracellular RCK1 domain serve as the H^+ sensors of the Slo1 BK channel. Activation of the channel by H^+ requires electrostatic interactions between the histidine residues and a nearby negatively charged residue involved in the channel's high-affinity Ca^{2+} sensitivity. Reciprocally, His365 and His394 also participate in the Ca^{2+}-dependent activation of the channel, functioning as Ca^{2+} mimetics once protonated. Therefore, a common motif in the RCK1 domain mediates the stimulatory effects of both H^+ and Ca^{2+}, and provides a basis for the bidirectional coupling of cell metabolism and membrane electrical excitability.

Normal functions of excitable cells, such as neurons and muscle cells, critically depend on an intimate and finely tuned regulation of membrane excitability by the cellular metabolic state. The metabolism, in turn, is reciprocally influenced by homeostasis of intracellular ions, and dysregulation of the ion concentrations accompanies many forms of abnormal excitability such as excitoxicity following ischemia/hypoxia [1] and also in neurodegenerative diseases [2]. Among the intracellular ion species, Ca^{2+} and H^+ are particularly important, functioning in an intertwined manner; H^+ can interfere with numerous Ca^{2+}-dependent processes and alters the intracellular Ca^{2+} concentration ($[Ca^{2+}]_i$) [3–5] and, in turn, alterations in $[Ca^{2+}]_i$ modulate the intracellular H^+ homeostasis [6].

One of the key coupling mechanisms between the cellular metabolism and electrical excitability is the Slo1 (also known as KCNMA1) BK channel [7,8]. The two distinguishing features of the channel, large conductance and synergic activation by membrane depolarization and intracellular Ca^{2+}, allow the channel to exert a negative feedback influence on cellular excitability under many physiological conditions, especially in neurons and muscle cells [9]. Consistent with this functional role, opening of BK channels often plays a cell-protective role against excitoxicity following hypoxia/ischemic insults [10,11].

As in other voltage-gated K^+ channels, four pore-forming Slo1 subunits form a functional BK channel complex, frequently with up to four auxiliary β subunits in a tissue-specific manner [12]. The transmembrane segments with its N-terminus facing the extracellular side contain the

*To whom correspondence should be addressed. E-mail: hoshi@hoshi.org.

AUTHOR CONTRIBUTIONS
Designed research: SH, SHH, TH; Performed research: SH, RX, TH; Analyzed data: SH, SHH, TH; Wrote the paper: SH, SHH, TH.

voltage sensor, and the large cytoplasmic domain is postulated to possess multiple divalent cation sensors within a putative cytoplasmic structured termed a “gating ring”, most probably comprised of four sets of dimers made of RCK1 (regulator of conductance for K^+) and RCK2 domains [13,14]. The octameric gating ring is considered to expand when Ca^{2+} binds to the putative high-affinity divalent cation sensor in the RCK1 domain and/or the Ca^{2+} bowl in the RCK2 domain near the distal C-terminus [15]. This ligand binding then facilitates opening of the channel’s gate [15] perhaps by increasing the tension on the spring-like linker segment between the gate and the RCK domains [16]. While many aspects of the Ca^{2+}-dependent activation of the channel, such as the molecular and biophysical characteristics of the Ca^{2+} sensors, remain elusive, electrophysiological studies collectively suggest that Ca^{2+} facilitates activation of the voltage sensor and opening of the gate so that the channel opens more frequently at more negative voltages [15,17]. This allosteric gating of the BK channel is modulated by a variety of intracellular signaling events, and the RCK1/RCK2 domains contain multiple sites critical for modulation of the BK channel such as that by oxidation [18], heme binding [19,20], and phosphorylation [21].

Intracellular H^+ is also a potent modulator of BK channel function [22–24]. While some conflicting reports exist whether native BK channels are stimulated or inhibited by a decrease in intracellular pH (pH_i), recent evidence shows that, unlike most other K^+ channels, Slo1 BK channels measured under defined conditions are robustly activated by a decrease in pH_i near the physiological level [22,23]. This stimulatory effect of low pH_i may be pathophysiologically significant in early stages of hypoxia/ischemia during which pH_i typically falls by 0.5 to 1 unit [1]. Despite the potential physiological and pathophysiological relevance, the molecular mechanism of the Slo1 BK channel activation by low pH_i has remained elusive. Our study presented here using human Slo1 BK channels reveals that each Slo1 subunit has a common molecular sensing domain for Ca^{2+} and H^+ containing two histidine residues and a negatively-charged residue and that the electrostatic interactions encompassing these residues is altered by H^+ or by Ca^{2+} to facilitate opening of the channel. Therefore, the multi-ligand sensor pockets in the Slo1 BK channel provide a direct molecular mechanistic link between the cellular excitability and metabolism.

RESULTS

Low intracellular pH activates native and recombinant BK channels

The activity of native Slo1 BK channels in rat aortic smooth muscle cells substantially increased when pH_i was lowered from 7.2 to 6.2 (Fig. 1a). The channel open probability and mean open duration at –40 mV in the presence of 200 nM $[Ca^{2+}]_i$ increased by 13.3 ± 2.8 and 3.2 ± 0.8 fold, respectively, without any effect on the single-channel current size. In contrast, a decrease in extracellular pH from 7.2 to 6.2 did not produce any significant effect (data not shown). The stimulatory effect of low pH_i was observed not only for recombinant human Slo1 (hSlo1) BK channels [23] but also for Slo1 channels from the fruit fly *Drosophila melanogaster* (dSlo1) and the cockroach *Periplaneta americana* (pSlo1; Fig. 1b), suggesting that the underlying molecular machinery is conserved in Slo1 channels from different species and resides in the pore-forming Slo1 α subunit of the BK channel. To identify whether the β1 subunit, the predominant type of auxiliary β subunits in vascular smooth muscle cells, has any modulating effect, we compared the effects of a pH_i decrease on heterologously-expressed hSlo1 and hSlo1+β1 channels. A decrease in pH_i by 1 unit from 7.2 prominently increased the macroscopic hSlo1 and hSlo1+β1 K^+ currents and shifted the conductance-voltage (G-V) curve to the negative voltage by about 50 mV in both types of channels (Fig. 1c). The simulation effect of H^+ was concentration dependent with an apparent EC_{50} of ~0.3 ⌠M or pH 6.5 (Fig. 1d) [23]. In addition to the leftward shift in G-V, lowering pH_i noticeably accelerated activation kinetics and slowed deactivation kinetics of the channel (Supplementary Fig. 1) [23].

Two histidine residues in the RCK1 domain mediate the H^+ sensitivity

Activation of Slo1 channels from diverse species by low pH_i (Fig. 1b) and the previous findings that the leftward G-V shift has an EC_{50} value of pH_i=6.5 [23] and that the shift is antagonized by the histidine modifier diethyl pyrocarbonate [23] collectively suggest that the stimulatory effect of low pH_i is mediated by conserved histidine residues in Slo1 accessible from the cytoplasmic side. Each hSlo1 subunit contains 12 conserved histidine residues, most of which are located in the large cytoplasmic C-terminal domain. In particular, the putative RCK1 and RCK2 domains contain 10 histidines (Fig. 2a). Each of the conserved histidine residues was replaced with arginine and the resulting mutants were assayed for their pH_i sensitivity using the shift of the G-V curve ($\Delta V_{0.5}$) observed when pH_i was lowered from 7.2 to 6.2 (Fig. 2b). A decrease in pH_i from 7.2 to 6.2 in the absence of Ca^{2+} in the intracellular solution causes a –50 mV shift in $V_{0.5}$ for the wild-type channel (Fig. 2b). We found that among the single histidine-to-arginine mutations examined, mutation of His365 and His394 located in the RCK1 domain significantly diminished the pH_i sensitivity (Fig. 2b, c). The $\Delta V_{0.5}$ value for the mutant H365R was –14.0 ± 1.0 mV and for the mutant H394R, it was –28.2 ± 2.0 mV ($P < 0.01$) or about 28% and 56% of the shift observed in the wild-type channel, respectively. When the two mutations were present concurrently (H365R:H394R), the $V_{0.5}$ shift by lowering pH_i from 7.2 to 6.2 was completely eliminated ($P < 0.01$). A greater decrease in pH_i to 5.7 and an increase in pH_i to 7.7 were without any effect (data not shown). Mutation of the two histidine residues to alanine (H365A:H394A) also disrupted the pH_i sensitivity ($P < 0.01$). Moreover, in these double mutants, the pH_i decrease failed to alter the kinetics of activation and deactivation (Fig. 2c; Supplementary Fig. 1).

Mutation of His616 located in the putative linker segment between the RCK1 and RCK2 domains (H616R) severely compromised the electrophysiological expression level and we could not obtain any macroscopic currents, even at 300 mV at high $[Ca^{2+}]_i$. However, single-channel measurements verified that the mutant H616R retained a pH_i sensitivity indistinguishable from that of the wild-type channel (Supplementary Fig. 2).

To infer about the physicochemical characteristics of His365 essential for the low pH_i sensitivity of the Slo1 channel, the histidine was substituted with a variety of amino acids. None of the mutants (Arg, Lys, Ala, Asn, Gln, Glu, or Asp at position 365) showed the pH_i sensitivity comparable to that of the wild-type channel; the $\Delta V_{0.5}$ values were about –15 mV, only 30% of the shift observed in the wild-type channel (Fig. 3a, b). Likewise, at position His394, substitution with Arg or Ala equally diminished the pH_i sensitivity (Fig. 3a, c). The mutagenesis results therefore suggest that the full wild-type like pH_i sensitivity requires histidine at positions 365 and 394.

The pK_a value of the imidazole side chain of histidine is often around 6 to 7 and lowering pH_i from 7.2 to 6.2 is expected to render the side chain positively charged to a greater extent. It may be reasoned that it is the presence of a positive charge at position 365 that in part shifts the voltage dependence of channel activation to the negative direction. According to this idea, $V_{0.5}$ of the channel with Lys and Arg at position 365 at pH_i=7.2 should resemble that of the wild-type channel with histidine at pH_i=6.2. This prediction is in part born out by comparison of the $V_{0.5}$ values of the mutants with different amino acids at position 365 at pH_i=7.2 (Fig. 3d). The $V_{0.5}$ values in the mutants H365R and H365K were in fact more negative than those of other mutants and similar to that of the wild-type channel at pH_i=6.2. The full pH_i sensitivity of the Slo1 channel thus requires histidine at positions 365 and 394 and the charge status of the imidazole side chain modulated by pH_i plays an essential role.

Electrostatic interactions are involved in the pH_i sensitivity

The mutagenesis results led us to hypothesize that an electrostatic mechanism underlies the pH_i-induced activation of the BK channel; protonated His365 and His394 in Slo1 at low pH_i electrostatically interact with nearby residues to facilitate channel activation. To test this idea, the pH_i sensitivity of the wild-type Slo1 channel was measured using internal solutions with varying ionic strengths; high ionic strength solutions should diminish the negative shift in $V_{0.5}$ normally observed with lowering pH_i. Consistent with this prediction, the mean $\Delta V_{0.5}$ value observed on lowering pH_i from 7.2 to 6.2 became progressively smaller with increasing ionic strengths (Fig. 4a, b).

High ionic strength solutions may slightly increase the pK_a value of the histidine side chain [25] so that the range of the pH_i sensitivity of the channel is shifted higher. This possibility can be discounted because increasing pH_i from 7.2 to 7.7 failed to alter the voltage dependence of the channel activation in both high and normal ionic solutions, indicating that any change in pK_a of the imidazole side chain by the ionic strength manipulations made a negligible contribution. Addition of sucrose, a non-electrolyte, did not affect the pH_i sensitivity (data not shown). Taken together, the above results suggest that electrostatic interactions involving His365 and His394 are critical in the pH_i-mediated regulation of the Slo1 BK channel.

Asp367 in the RCK1 Ca^{2+} sensor is important for the pH_i sensitivity

A high-resolution atomic structure of the Slo1 channel is not yet available but the amino-acid sequence in the RCK1 domain of Slo1 is relatively similar to that of the bacterial K^+ channel MthK whose high-resolution structures are known [13,26]. A homology model of the Slo1 RCK1 domain based on an MthK structure [7] suggests that the two histidine residues critical for the pH_i sensitivity, His365 and His394, may be in close proximity of the negatively-charged residues Asp362, Asp367, Asp369, Asp370, Glu374, Glu399, and Asp420 (Fig. 5a). Some of these negatively-charged residues are important for the divalent cation sensitivity of the Slo1 channel, probably forming a high- and a low-affinity divalent cation sensors [27–29]. The possible proximity of His365/His394 to the negatively-charged residues involved in the divalent cation sensitivity suggests that some of these negative charges might be the electrostatic interaction partners of protonated His365 and/or His394. If so, neutralization of the negatively-charged residues should also disrupt the pH_i sensitivity of the channel. Neutralization of Glu374, Asp369, Asp370, or Asp420 failed to alter the $\Delta V_{0.5}$ caused by lowering pH_i from 7.2 to 6.2 (Fig. 5c). In contrast, $\Delta V_{0.5}$ was significantly diminished by the triple mutation D362A:D367A:E399A ($P < 0.01$; Fig. 5b, c), which is known to interfere with the Ca^{2+} sensitivity mediated by the RCK1 domain of the channel [27,29]. Among the three negatively charged residues, only Asp367 plays a critical role in the pH_i sensitivity of the channel because, when mutated separately, neutralization of Asp367 but not Asp362 or Glu399 noticeably diminished the $\Delta V_{0.5}$ in response to a decreased in pH_i (Fig. 4b, c). However, the mutation D367A does not completely eliminate the pH_i sensitivity, leaving open the possibility that other structural components, including backbone dipoles, electrostatically interact with His365 and His394.

His365 and His394 are also involved in Ca^{2+}-dependence of Slo1

Our results show that the pH_i sensitivity of the Slo1 channel requires His365 and His394 as well as Asp367, one of the residues in the RCK1 domain implicated for high-affinity Ca^{2+} sensing [27,29]. The involvement of Asp367 in both the pH_i and Ca^{2+} sensing of the channel suggest that His365 and His394 may in turn participate in the channel's Ca^{2+} sensing. In the wild-type channel, increasing $[Ca^{2+}]_i$ to 200 μM shifted $V_{0.5}$ to the negative direction by ~200 mV (Fig. 6a). The triple mutation D362A:D367A:E399A, which disrupts the high-affinity Ca^{2+} sensor in the RCK1 domain [27], reduces the $V_{0.5}$ shift caused by 200 μM $[Ca^{2+}]_i$ by half to ~100 mV with the remaining Ca^{2+} sensitivity mediated by the Ca^{2+}-bowl segment at the

distal C-terminus [27,29]. Comparison of the $\Delta V_{0.5}$ values at different $[Ca^{2+}]_i$ (Fig. 6a) showed that the two histidine double mutants H365R:H394R and H365A:H394A, neither of which showed any appreciable pH_i sensitivity, also had noticeably diminished sensitivity to $[Ca^{2+}]_i$; the $V_{0.5}$ shift by 200 μM $[Ca^{2+}]_i$ was about 100 mV or 50% of that found in the wild-type channel. The dependence of $V_{0.5}$ on $[Ca^{2+}]_i$ in the pH_i-insensitive histidine mutants in fact closely resembled that of the triple mutant D362A:D367A:E399A with the disrupted RCK1 Ca^{2+} sensor.

In addition to Ca^{2+}, intracellular Mg^{2+} also activates the Slo1 channel, and Glu374 and Glu399 in the RCK1 domain, potentially near His365 and His394 (Fig. 6b), form a low-affinity divalent cation-sensing site that transduces alterations in $[Mg^{2+}]_i$ [27–29]. Therefore, we examined whether His365 and His394 are involved in the channel's low-affinity divalent cation ion sensitivity. The Mg^{2+}-dependent activation of the double mutant H365R:H394R was indistinguishable from that of the wild-type channel (Fig. 6b). Similar results were also obtained with the double mutant H365A:H394A (data not shown).

DISCUSSION

Slo1 BK channels constitute an important element linking cellular metabolism and membrane excitability in part because of the synergic activation by intracellular Ca^{2+} and membrane depolarization. Recent results have shown that Slo1 BK channels are also activated by intracellular H^+, a key regulator of cellular metabolism, thereby providing an additional coupling pathway between cell metabolism and membrane excitability. Here we have elucidated the mechanism of such signaling linkage provided by the Slo1 channel and intracellular H^+. Two histidine residues, His365 and His394 located in the RCK1 domain are essential for the pH_i sensitivity of the Slo1 BK channel. Protonated His365 and His394 electrostatically interact with Asp367 and potentially with other charged residues and/or dipoles to selectively transduce changes in $[Ca^{2+}]_i$ and $[H^+]_i$ to allosterically facilitate opening of the channel gate.

The mutagenesis results presented here suggest that histidine with the imidazole side chain at positions 365 and 394 is the only naturally occurring amino acid that supports the pH_i-dependent activation of the Slo1 channel. Furthermore, substitution of His365 and His394 with arginine or lysine alters the voltage dependence of the channel at normal pH_i to resemble that of the wild-type channel at low pH_i at which His365 and His394 are expected to be protonated. These observations together show that His365 and His394 represent the primary H^+ sensors of the channel required to facilitate its activation.

The H^+ sensors His365 and His394, when protonated, electrostatically interact with Asp367 as evidenced by the results of the ionic strength manipulations and the charge-neutralization mutation of aspartic acid at position 367. The exact spatial arrangement of these interacting residues is not yet clear because of the lack of detailed structural information. However, the residues are likely to be arranged within ~10 to 15 Å of each other based on the typical effective range of long-distance electrostatic interactions [30]. A homology model of the Slo1 RCK1 domain developed by Latorre and Brauchi [7] (Fig. 5a) suggests a distance of ~7 Å between the side chains of His365 and Asp367 and of ~20 Å between those of His394 and Asp367.

In addition to Asp367, other charged residues and/or dipoles, such as carbonyl oxgens, must electrostatically interact with His365 and His394 for neutralization of Asp367 alone eliminate only ~50% of the pH_i sensitivity. Asp367 is part of the high-affinity divalent cation sensor in the RCK1 domain of the channel, which under physiological conditions, transduces $[Ca^{2+}]_i$ [27,29]. Therefore, we suggest that His365, His394 and Asp367 form a bi-functional ligand-

sensing subdomain for intracellular H^+ and Ca^{2+} such that mutation of the aforementioned residues alters the sensitivity to both H^+ and Ca^{2+}.

The electrostatic mechanism of the H^+-dependent activation of the channel involving His365 and His394 provides unexpected insights into the properties of the high-affinity divalent cation sensor in the RCK1 domain. Mutation of Asp367 or Met513 in this domain interferes with the overall high-affinity divalent cation sensitivity of the channel [27,29,31]; however, complete and detailed characteristics of the sensors have not been elucidated. Our study here shows that the two histidines residues are integral components of the high-affinity divalent cation sensor. The electrostatic interaction of the protonated side chains of His365 and His394 with Asp367 at low pH_i functionally and partly mimics the interaction of Ca^{2+} with Asp367; H^+ of the His365/His394 imidazole side chain acts as a Ca^{2+} mimic for Asp367. The contributions of His365 and His394 to the H^+-dependent activation of the channel may be energetically independent of each other because the effects of the His365 and His394 mutations on the voltage dependence are additive. This conclusion must be considered somewhat tentative, however, because multiple gating transitions contribute to determination of the data description parameter $V_{0.5}$.

While both H^+ and Ca^{2+} shift the voltage dependence of the channel to the negative direction, thus providing a stimulatory influence on the channel, some differences in their actions on the channel do exist. The maximal shift in the voltage dependence induced by high concentrations of Ca^{2+}, about –200 mV, is appreciably larger than that by H^+. This difference occurs because the overall high-affinity Ca^{2+} sensitivity of Slo1 arises from two distinct but relatively equipotent sensors, the RCK1 sensor and the Ca^{2+} bowl [32], while the H^+ sensitivity is mediated only by the RCK1 sensor. The Ca^{2+} bowl does not contribute to the H^+ sensitivity, thus further illustrating functional differences between the two high-affinity Ca^{2+} sensors. Even within the RCK1 Ca^{2+}/H^+ sensor subdomain, clear functional specializations are observed. For example, His365, His394 and Asp367 transduce both Ca^{2+} and H^+ but Asp362 near the high-affinity Ca^{2+} sensor in the RCK1 domain [27,29], does not contribute to the pH_i sensitivity. The true binding affinity of the subdomain to H^+ and Ca^{2+} is not known, but the EC_{50} values of the channel activation for H^+ and Ca^{2+} based on ionic current measurements are about 0.35 μM [23] and ~10 μM [33], respectively, suggesting that the Slo1 channel may be considered more sensitive to H^+ than to Ca^{2+}.

The cytoplasmic gating ring domain of the Slo1 is considered to be structurally similar to that of the prokaryotic channel MthK [14,34]. Yet, in clear contrast to the H^+-stimulated gating of Slo1 described here, the MthK channel activity is profoundly inhibited by H^+[26]. At low pH_i (e.g., 6.2), the gating ring of MthK disassembles into four dimers [35] and the channel fails to open, even in the presence of 10 mM $[Ca^{2+}]$ [26]. In the Slo1 channel, H^+ essentially acts as a Ca^{2+} mimetic for the RCK1 Ca^{2+} sensor and it is highly unlikely that the Slo1 gating ring structure undergoes pH-dependent assembly and disassembly as observed in the MthK channel. The pH_i-sensitivity of MthK has been suggested to require His193 located in its otherwise hydrophobic octamer assembly interface [26]. His193 is poorly conserved among RCK domains [26] and it is equivalent to M442 in the Slo1 channel [34], distinct from His365 and His394 required for the H^+-stimulated gating. Conversely, the residues equivalent to His365 and H394 do not exist in MthK (Fig. 2a). Thus, while MthK and Slo1 share a similar cytoplasmic structural organization, the two channels employ distinct mechanisms to transduce intracellular pH.

The high sensitivity of the Slo1 BK channel to changes in pH_i renders this channel very well suited for coupling membrane excitability/neuronal transmission and cellular metabolism. The cellular metabolic state and pH_i are intimately and reciprocally linked, and H^+ may be viewed as a metabolic intracellular messenger [36,37]. Accordingly, the H^+ and Ca^{2+} sensitivity of the Slo1 BK channel conferred by His365, His394 and Asp367 is likely to have physiological implications. Fluctuations in pH_i, under both physiological and pathophysiological conditions,

are typically accompanied by changes in $[Ca^{2+}]_i$. For example, intense neuronal firing leads to a noticeable decrease in pH_i [6,38]. Pathophysiologically, malignant hyperthermia and hypercapnia decrease pH_i [39,40]. Furthermore, cerebral ischemia decreases pH_i rapidly within a few minutes from by 0.5 to 1 unit [1], large enough to noticeably activate Slo1 BK channels. Concurrently with the increase in $[H^+]_i$, ischemia frequently causes a substantial increase in $[Ca^{2+}]_i$, in part through activation of Ca^{2+}-permeant glutamate receptor channels, possibly leading to excitoxicity [41]. Increases in both $[H^+]_i$ and $[Ca^{2+}]_i$ activate Slo1 BK channels, but the two ligand-dependent activation mechanisms may play differential roles in blunting the extent of hyperexcitability caused by Ca^{2+}. It may be speculated that the H^+-mediated activation of the Slo1 BK channel has a feed-forward anticipatory role while the Ca^{2+}-dependent activation of the channel has a feedback role in regulation of the membrane excitability.

K^+ channels are an exceptionally diverse family of ion channels. However, only a very small number of the channels are activated by intracellular H^+. TREK-1, a two-pore domain voltage-independent leak K^+ channels with four transmembrane segments, is one example [42]. Among the voltage-dependent K^+ channels, the Slo1 BK channel is unique in that intracellular H^+ enhances its ionic current [22,23]. Both the permeation and gating properties of the Slo1 channel are well suited to transduce changes in pH_i. As shown in this study, low pH_i prominently shifts the voltage dependence of activation to the negative direction to facilitate channel opening. Furthermore, unlike most other K^+ channels, the single-channel conductance of the Slo1 channel, especially at physiological voltages, is resistant to pore blocking by intracellular H^+[43]. In Shaker and other voltage-gated K^+ channels, lowering pH_i to 6.4 decreases the single-channel current size by about 50% without affecting their voltage dependence of activation [44]. The unusual H^+-activated gating based the electrostatic interactions encompassing histidine and aspartic acid residues in the RCK1 domain and the H^+-resistant permeation characteristics of the Slo1 BK channel contribute to its role as an important coupling mechanism between the cell metabolic state and membrane excitability [8]. To serve a variety of physiological needs, cells express a diverse complement of K^+ channels, most of which are inhibited by H^+. Inclusion of Slo1 BK channels activated by H^+ and Ca^{2+} in the proteome permits fine-tuning of the membrane excitability according to their metabolic state.

METHODS

Channel expression and cell isolation

Human (KCNMA1; U11058), *Drosophila* (M96840) [45] and *Periplaneta* Slo1 (AF452164) 45 in the expression vectors pCI-neo (Promega), pcDNA3 (Invitrogen) and pcDNA3, respectively, were transiently expressed in HEK tsA cells using FuGENE 6 (Roche) as described 19. In some experiments, human Slo1 and β1 (KCNMB1; U38907) in pEGFP-N1 (Clontech) with 1:1 weight ratio were transfected together. We constructed the mutant channels using a PCR–based mutagenesis method (Stratagene). Other constructs used are described in the legends. Cultured rat aortic smooth muscle cells were prepared as described 46.

Electrophysiology and data analysis

Macroscopic and single–channel ionic currents were recorded from excised inside-out membrane patches at room temperature [19]. Patch electrodes (Warner) had a typical resistance of 1.5 – 2.0 MΩ and the series resistance, 90% of the initial input resistance, was electronically compensated in macroscopic current measurements. Macroscopic capacitive and leak currents were subtracted using a *P*/6 protocol. The current signal was filtered at 10 kHz through the built-in filter of the patch-clamp amplifier (AxoPatch 200A; Axon) and digitized at 100 kHz using an ITC-16 AD/DA interface (Instrutech). The results were analyzed as previously described using IGOR Pro (Wavemetrics) [19]. Statistical comparisons were performed using

the unpaired or paired *t* test, as appropriate. Comparison of more than two groups was performed using ANOVA followed by a Tukey HSD test [47] as implemented in IGOR Pro. Statistical significance was assumed at $P \leq 0.05$ and all data are presented as mean ± s.e.m.

Solutions

The extracellular solution for rat aortic smooth cells contained (in mM): 134 NaCl, 6 KCl, 1 $MgCl_2$, 2 $CaCl_2$, 10 Glucose, 10 HEPES, pH 7.4 with NaOH. The extracellular solution for HEK tsA cells contained (in mM): 140 KCl, 2 $MgCl_2$, 10 HEPES, pH 7.2 with *N*-methyl-*D*-glucamine (NMDG). To compare Slo1 currents at different pH_i in the virtual absence of Ca^{2+}, the intracellular solution contained (in mM): 140 KCl, 11 EDTA and either 10 HEPES (NMDG) for pH_i 7.2 or 10 MES (NMDG) for pH_i 5.7, 6.2 and 6.7. These solutions were assumed to have $[Ca^{2+}]$=10 nM [48]. EDTA was selected because its chelating ability is less sensitive to changes in pH than EGTA. BAPTA was not used in the study as it may have a direct blocking action on the Slo1 channel [23]. The concentrations of NMDG in the above internal solutions were from 3 to 20 mM and, at these concentrations, no effect on the Slo1 channel activity was observed. Free Ca^{2+} concentrations ($[Ca^{2+}]$) were calculated using Patcher's Power Tools for Electrophysiologists (http://www.mpibpc.gwdg.de/abteilungen/140/software/). The pH = 7.2 solutions with different $[Ca^{2+}]$ were prepared as descried [49] using EGTA or EDTA (for $[Ca^{2+}]$ = ~10 nM (no added Ca^{2+})), HEDTA ($[Ca^{2+}]$ = 200 nM – 5 μM) or without any chelator ($[Ca^{2+}$=]≥200 μM).

Supplementary Material

Refer to Web version on PubMed Central for supplementary material.

Acknowledgments

We thank Dr. M. L. Garcia for the original Slo1 construct and Drs. Latorre and Brauchi for the structural model. Supported in part by NIH and SFB 604 (TP A4).

References

1. Lipton P. Ischemic cell death in brain neurons. Physiol Rev 1999;79:1431–568. [PubMed: 10508238]
2. Kann O, Kovacs R. Mitochondria and neuronal activity. American journal of physiology 2007;292:C641–57. [PubMed: 17092996]
3. Higo T, et al. Subtype-specific and ER lumenal environment-dependent regulation of inositol 1,4,5-trisphosphate receptor type 1 by ERp44. Cell 2005;120:85–98. [PubMed: 15652484]
4. Austin C, Wray S. Interactions between Ca^{2+} and H^+ and functional consequences in vascular smooth muscle. Circ Res 2000;86:355–63. [PubMed: 10679489]
5. Yao H, Haddad GG. Calcium and pH homeostasis in neurons during hypoxia and ischemia. Cell Calcium 2004;36:247–55. [PubMed: 15261480]
6. Chesler M. Regulation and modulation of pH in the brain. Physiol Rev 2003;83:1183–221. [PubMed: 14506304]
7. Latorre R, Brauchi S. Large conductance Ca^{2+}-activated K^+ (BK) channel: activation by Ca^{2+} and voltage. Biological research 2006;39:385–401. [PubMed: 17106573]
8. Toro L, Stefani E. Calcium-activated K^+ channels: metabolic regulation. J Bioenerg Biomembr 1991;23:561–76. [PubMed: 1917909]
9. Vergara C, Latorre R, Marrion NV, Adelman JP. Calcium-activated potassium channels. Curr Opin Neurobiol 1998;8:321–9. [PubMed: 9687354]
10. Xu W, et al. Cytoprotective role of Ca^{2+}- activated K^+ channels in the cardiac inner mitochondrial membrane. Science 2002;298:1029–33. [PubMed: 12411707]

11. Gribkoff VK, et al. Targeting acute ischemic stroke with a calcium-sensitive opener of maxi-K potassium channels. Nat Med 2001;7:471–7. [PubMed: 11283675]
12. Tseng-Crank J, et al. Cloning, expression, and distribution of functionally distinct Ca^{2+}-activated K^+ channel isoforms from human brain. Neuron 1994;13:1315–30. [PubMed: 7993625]
13. Jiang Y, et al. Crystal structure and mechanism of a calcium-gated potassium channel. Nature 2002;417:515–22. [PubMed: 12037559]
14. Jiang Y, Pico A, Cadene M, Chait BT, MacKinnon R. Structure of the RCK domain from the *E. coli* K^+ channel and demonstration of its presence in the human BK channel. Neuron 2001;29:593–601. [PubMed: 11301020]
15. Magleby KL. Gating mechanism of BK (Slo1) channels: so near, yet so far. J Gen Physiol 2003;121:81–96. [PubMed: 12566537]
16. Niu X, Qian X, Magleby KL. Linker-gating ring complex as passive spring and Ca^{2+}-dependent machine for a voltage- and Ca^{2+}-activated potassium channel. Neuron 2004;42:745–56. [PubMed: 15182715]
17. Horrigan FT, Aldrich RW. Coupling between voltage sensor activation, Ca^{2+} binding and channel opening in large conductance (BK) potassium channels. J Gen Physiol 2002;120:267–305. [PubMed: 12198087]
18. Tang XD, Santarelli LC, Heinemann SH, Hoshi T. Metabolic regulation of potassium channels. Annu Rev Physiol 2004;66:131–59. [PubMed: 14977399]
19. Tang XD, et al. Haem can bind to and inhibit mammalian calcium-dependent Slo1 BK channels. Nature 2003;425:531–5. [PubMed: 14523450]
20. Jaggar JH, et al. Heme is a carbon monoxide receptor for large-conductance Ca^{2+}-activated K^+ channels. Circ Res 2005;97:805–12. [PubMed: 16166559]
21. Schubert R, Nelson MT. Protein kinases: tuners of the BK_{Ca} channel in smooth muscle. Trends Pharmacol Sci 2001;22:505–12. [PubMed: 11583807]
22. Hayabuchi Y, Nakaya Y, Matsuoka S, Kuroda Y. Effect of acidosis on Ca^{2+}-activated K^+ channels in cultured porcine coronary artery smooth muscle cells. Pflügers Arch 1998;436:509–14.
23. Avdonin V, Tang XD, Hoshi T. Stimulatory action of internal protons on Slo1 BK channels. Biophys J 2003;84:2969–80. [PubMed: 12719228]
24. Church J, Baxter KA, McLarnon JG. pH modulation of Ca^{2+} responses and a Ca^{2+}-dependent K^+ channel in cultured rat hippocampal neurones. J Physiol (Lond) 1998;511:119–32. [PubMed: 9679168]
25. Lee KK, Fitch CA, Lecomte JT, Garcia-Moreno EB. Electrostatic effects in highly charged proteins: salt sensitivity of pK_a values of histidines in staphylococcal nuclease. Biochemistry 2002;41:5656–67. [PubMed: 11969427]
26. Ye S, Li Y, Chen L, Jiang Y. Crystal structures of a ligand-free MthK gating ring: insights into the ligand gating mechanism of K^+ channels. Cell 2006;126:1161–73. [PubMed: 16990139]
27. Xia XM, Zeng X, Lingle CJ. Multiple regulatory sites in large-conductance calcium-activated potassium channels. Nature 2002;418:880–4. [PubMed: 12192411]
28. Shi J, et al. Mechanism of magnesium activation of calcium-activated potassium channels. Nature 2002;418:876–80. [PubMed: 12192410]
29. Zeng XH, Xia XM, Lingle CJ. Divalent cation sensitivity of BK channel activation supports the existence of three distinct binding sites. J Gen Physiol 2005;125:273–86. [PubMed: 15738049]
30. Miksovska J, et al. Distant electrostatic interactions modulate the free energy level of QA- in the photosynthetic reaction center. Biochemistry 1996;35:15411–7. [PubMed: 8952493]
31. Bao L, Rapin AM, Holmstrand EC, Cox DH. Elimination of the BK_{Ca} channel's high-affinity Ca^{2+} sensitivity. J Gen Physiol 2002;120:173–89. [PubMed: 12149279]
32. Qian X, Niu X, Magleby KL. Intra- and intersubunit cooperativity in activation of BK channels by Ca^{2+} J Gen Physiol 2006;128:389–404. [PubMed: 17001085]
33. Cox DH, Cui J, Aldrich RW. Allosteric gating of a large conductance Ca-activated K^+ channel. J Gen Physiol 1997;110:257–81. [PubMed: 9276753]
34. Roosild TP, Miller S, Booth IR, Choe S. A mechanism of regulating transmembrane potassium flux through a ligand-mediated conformational switch. Cell 2002;109:781–91. [PubMed: 12086676]

35. Dong J, Shi N, Berke I, Chen L, Jiang Y. Structures of the MthK RCK domain and the effect of Ca^{2+} on gating ring stability. J Biol Chem 2005;280:41716–24. [PubMed: 16227203]
36. Takahashi KI, Copenhagen DR. Modulation of neuronal function by intracellular pH. Neurosci Res 1996;24:109–16. [PubMed: 8929916]
37. Kelly T, Church J. pH modulation of currents that contribute to the medium and slow afterhyperpolarizations in rat CA1 pyramidal neurones. J Physiol (Lond) 2004;554:449–66. [PubMed: 14608014]
38. Filosa JA, Dean JB, Putnam RW. Role of intracellular and extracellular pH in the chemosensitive response of rat locus coeruleus neurones. J Physiol (Lond) 2002;541:493–509. [PubMed: 12042354]
39. Decanniere C, Van Hecke P, Vanstapel F, Ville H, Geers R. Metabolic response to halothane in piglets susceptible to malignant hyperthermia: an in vivo ^{31}P-NMR study. J Appl Physiol 1993;75:955–62. [PubMed: 8226501]
40. Denton JS, McCann FV, Leiter JC. CO_2 chemosensitivity in *Helix aspersa*: three potassium currents mediate pH-sensitive neuronal spike timing. Am J Physiol Cell Physiol 2007;292:C292–304. [PubMed: 16928774]
41. Rothman SM, Olney JW. Excitotoxicity and the NMDA receptor. Trends Neurosci 1987;10:299–302.
42. Maingret F, Patel AJ, Lesage F, Lazdunski M, Honore E. Mechano- or acid stimulation, two interactive modes of activation of the TREK-1 potassium channel. J Biol Chem 1999;274:26691–6. [PubMed: 10480871]
43. Brelidze TI, Magleby KL. Protons block BK channels by competitive inhibition with K^+ and contribute to the limits of unitary currents at high voltages. J Gen Physiol 2004;123:305–19. [PubMed: 14981139]
44. Starkus JG, Varga Z, Schonherr R, Heinemann SH. Mechanisms of the inhibition of Shaker potassium channels by protons. Pflügers Arch 2003;447:44–54.
45. Derst C, et al. The large conductance Ca^{2+}-activated potassium channel (pSlo) of the cockroach *Periplaneta americana*: structure, localization in neurons and electrophysiology. The European journal of neuroscience 2003;17:1197–212. [PubMed: 12670308]
46. Tammaro P, Smith AL, Hutchings SR, Smirnov SV. Pharmacological evidence for a key role of voltage-gated K^+ channels in the function of rat aortic smooth muscle cells. Br J Pharmacol 2004;143:303–17. [PubMed: 15326038]
47. Zar, JH. Biostatistical analysis. Prentice Hall; Upper Saddle River, N. J: 1999.
48. Tang XD, et al. Oxidative regulation of large conductance calcium-activated potassium channels. J Gen Physiol 2001;117:253–74. [PubMed: 11222629]
49. Santarelli LC, Wassef R, Heinemann SH, Hoshi T. Three methionine residues located within the regulator of conductance for K^+ (RCK) domains confer oxidative sensitivity to large-conductance Ca^{2+}-activated K^+ channels. J Physiol (Lond) 2006;571:329–48. [PubMed: 16396928]
50. Long SB, Campbell EB, Mackinnon R. Crystal structure of a mammalian voltage-dependent Shaker family K^+ channel. Science 2005;309:897–903. [PubMed: 16002581]
51. Guex N, Peitsch MC. SWISS-MODEL and the Swiss-PdbViewer: an environment for comparative protein modeling. Electrophoresis 1997;18:2714–23. [PubMed: 9504803]

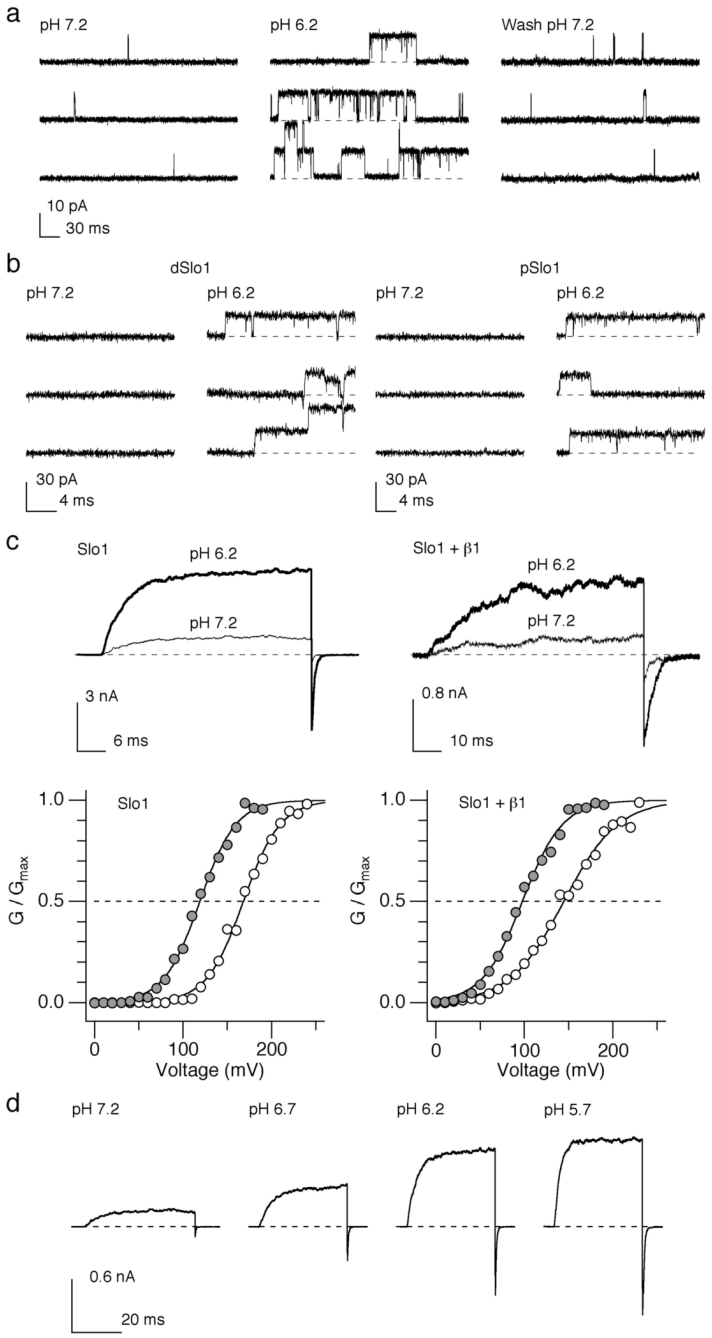

Figure 1.

Low pH_i enhances the native and recombinant BK channel activity. (**a**) Representative single-channel current openings in response to pulses from –80 to –40 mV from a rat aortic smooth muscle cell at pH_i=7.2, 6.2 and after wash at 7.2. (**b**) Representative openings elicited by pulses from 0 mV to 160 mV in membrane patches from HEK cells expressing *Drosophila melanogaster* Slo1 (dSlo1; *left*) and *Periplaneta americana* Slo1 (pSlo1; *right*). (**c**) Representative macroscopic current traces at pH_i=7.2 and 6.2 through by heterologously-expressed hSlo1 and hSlo1+β1 channels. The currents were activated by depolarization from 0 mV to 100 mV (hSlo1) and 70 mV (hSlo1+β1) in the absence of Ca^{2+}, respectively. Normalized G-V curves at pH_i=7.2 (open circles) and 6.2 (filled circles) are shown below the

current traces. The smooth curves represent Boltzmann fits. (**d**) Currents from hSlo1 channels elicited by pulses from 0 to 100 and then to –80 mV at the different pH_i indicated in the absence of Ca^{2+}.

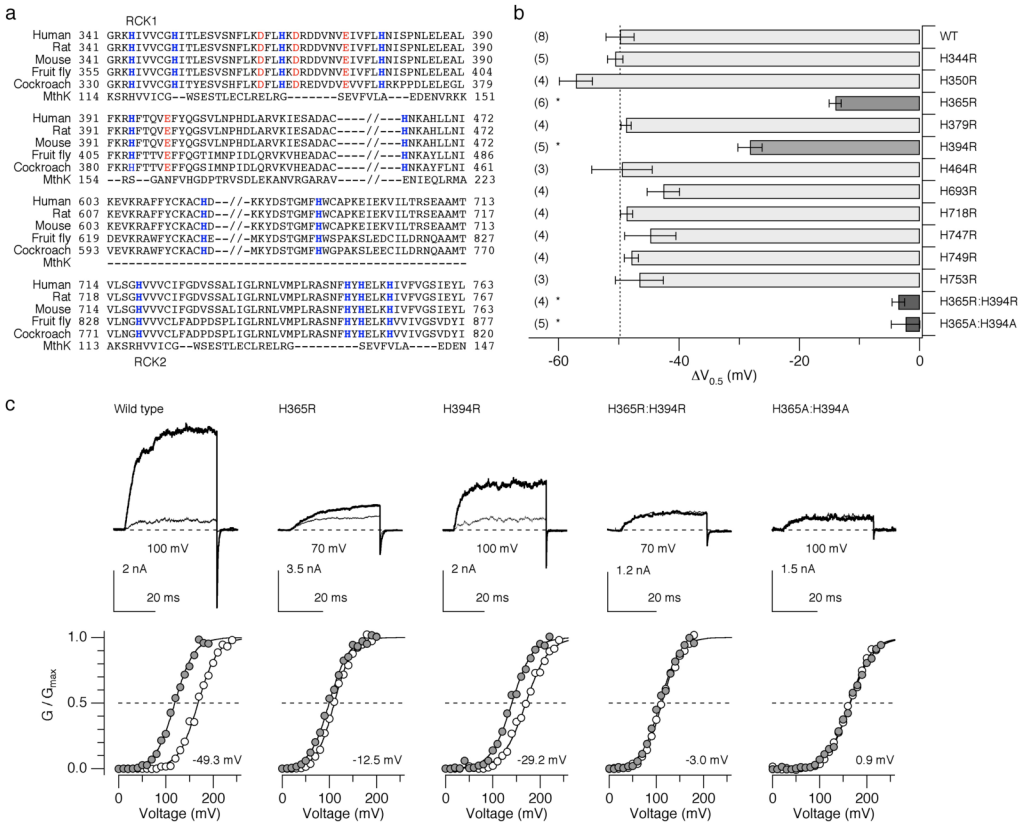

Figure 2.

Mutation of two histidine residues located in the RCK1 domain of hSlo1 abolishes the sensitivity to low pH_i. (**a**) Sequence alignment of the C-terminal intracellular domains of Slo1 from human (GI:507922), rat (rSlo1, GI:46396068), mouse (GI:18448948), the fruit fly *Drosophila melanogaster* (GI:115311626), and the American cockroach *Periplaneta americana* (GI:25991360). The MthK sequence is also shown aligned [34]. Histidine residues conserved among Slo1 are shown in blue. (**b**) Changes in $V_{0.5}$ caused by a decrease in pH_i from 7.2 to 6.2 in the wild-type and mutant channels in the absence of Ca^{2+} (also see Supplementary Table 1). * $P < 0.01$. Error bars represent s.e.m. (**c**) Representative currents recorded at pH_i=7.2 (thin sweeps) and 6.2 (thick sweeps) for the wild-type and select mutant Slo1 channels in the absence of Ca^{2+}. The currents were elicited by pulses from 0 to the voltages indicated where G/G_{max} is about 0.1 at pH_i=7.2. Normalized G-V curves at pH_i=7.2 (open circles) and 6.2 (filled circles) are shown below the current sweeps. The number in each graph represents $\Delta V_{0.5}$. The smooth curves are Boltzmann fits to the data.

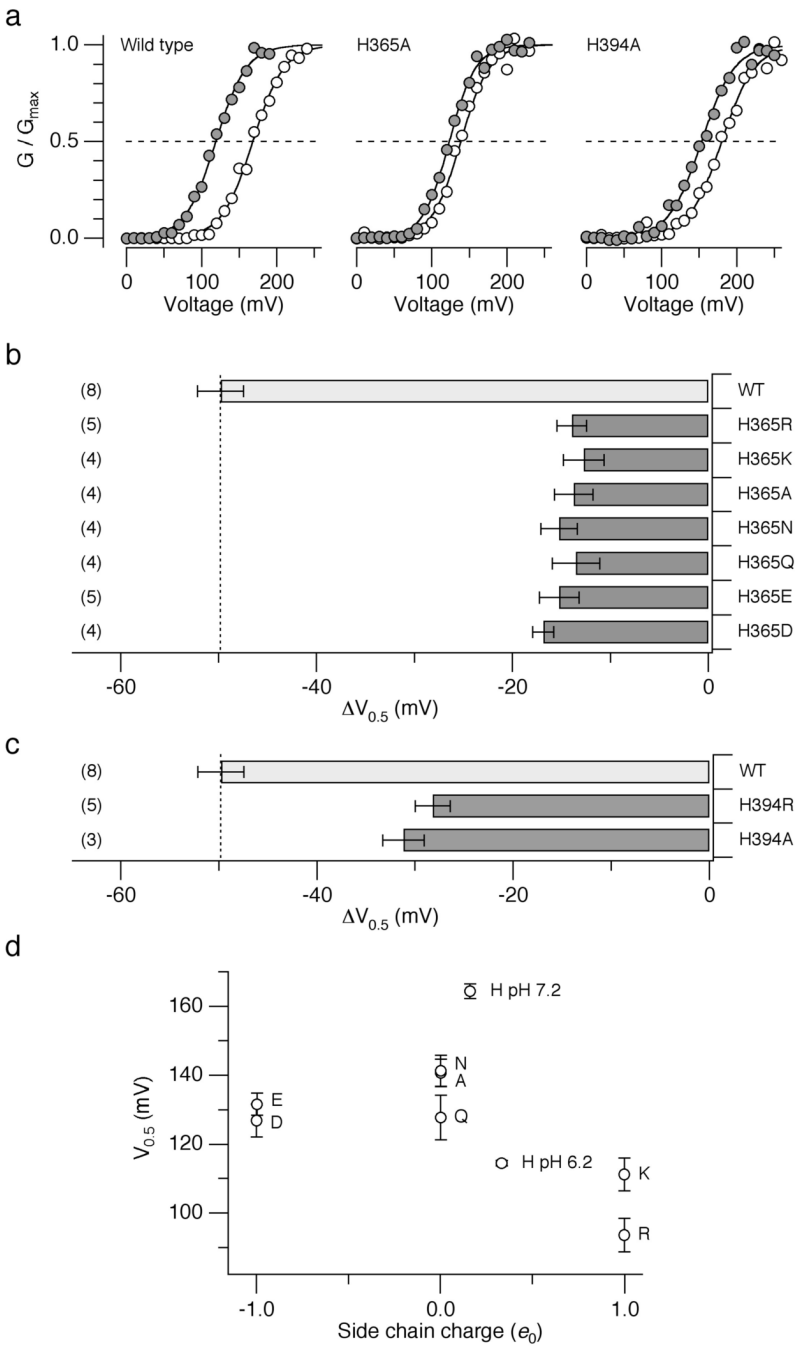

Figure 3.

Mutation of His365 and His394. (**a**) Representative G-V curves from the wild-type, H365A and His394 channels at pH_i=7.2 (open circles) and 6.2 (filled circles) in the absence of Ca^{2+}. (**b**) Mean $\Delta V_{0.5}$ values caused by lowering pH_i from 7.2 to 6.2 in the wild-type and the mutant channels with different amino acids at position 365. (**c**) Mean $\Delta V_{0.5}$ values caused by lowering pH_i from 7.2 to 6.2 in the wild-type and the mutant channels with different amino acids at position 394. (**d**) Mean $V_{0.5}$ values at pH_i=7.2 in the absence of Ca^{2+} from the mutant channels with different amino acids at position 365 as a function of the side chain charge status. Arg and Lys are assumed to be fully positively charged and Asp and Glu were assumed to be fully negatively charged. Ala, Asn, and Gln were assumed to have no net charge. The values for the

wild-type channels at pH_i=6.2 and 7.2 are also shown assuming that the side chain pK_a=6.5. Error bars represent s.e.m.

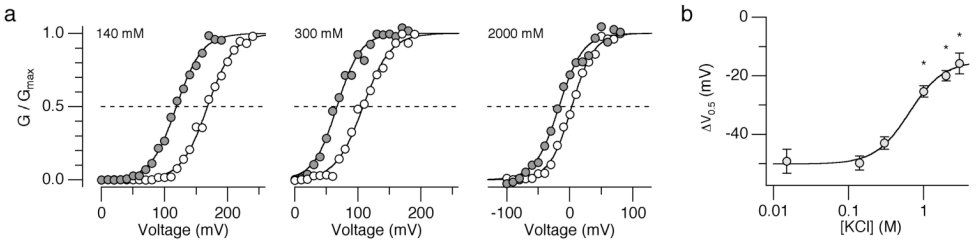

Figure 4.

High ionic strength solutions diminish $\Delta V_{0.5}$ caused by lowering pH_i from 7.2 to 6.2 in the absence of Ca^{2+}. (**a**) Representative G-V curves from the wild-type hSlo1 channels in different concentrations of KCl (mM). (**b**) $\Delta V_{0.5}$ values at different $[KCl]_i$. The curve represents the Hill equation fit. Error bars represent s.e.m. n = 3 to 8. * $P < 0.01$.

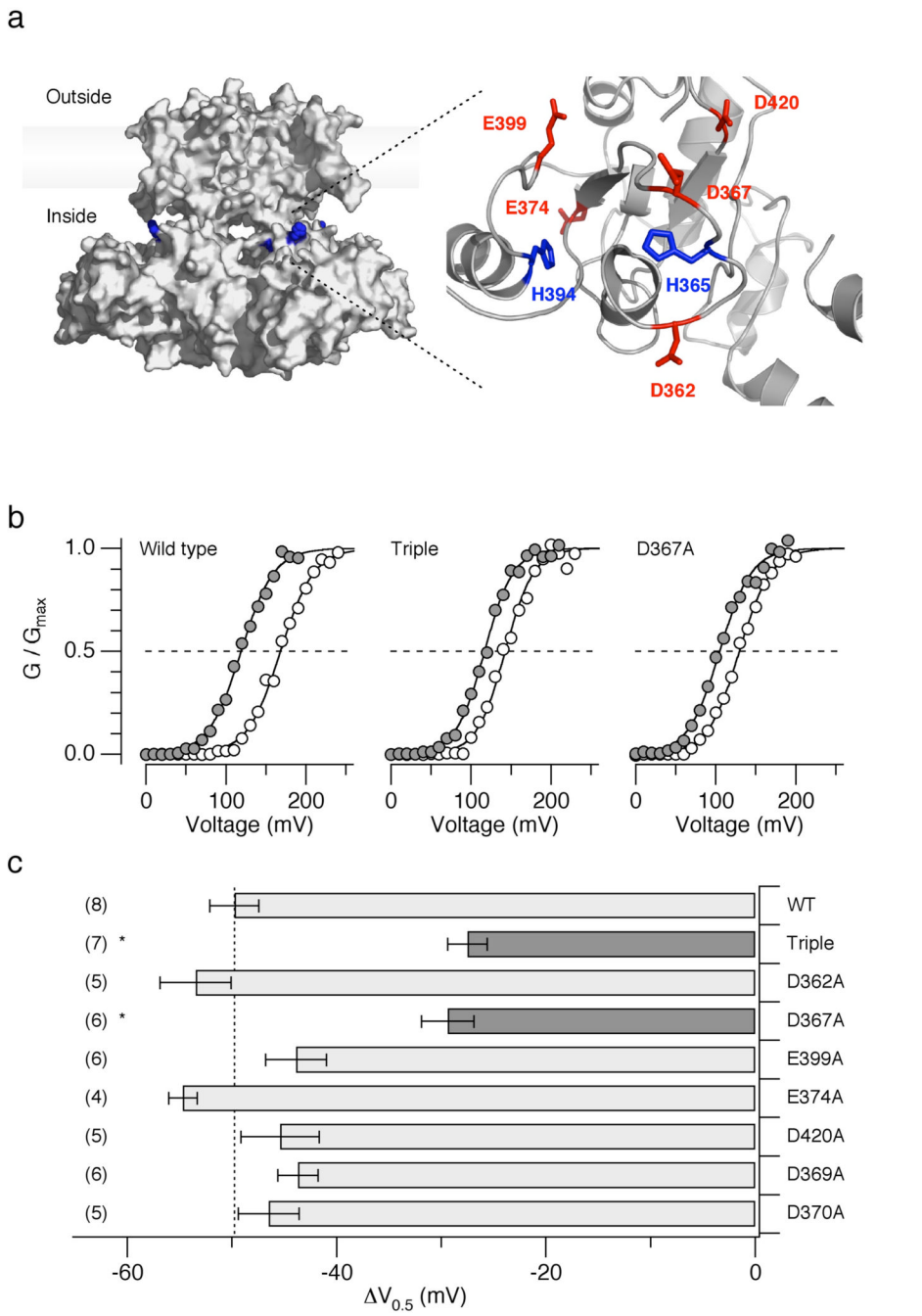

Figure 5.

Mutation of Asp367 diminishes the pH_i sensitivity. (**a**) A speculative overall structure of hSlo1 illustrating the locations of His365 and His394 (*left*) and a homology model of the Slo1 RCK1 domain (*right*). The hSlo1 sequence was aligned with those of Kv1.2 (2A79) [50] and of MthK (1LNQ) and the overall structure (*left*) was inferred [51]. The homology model of the RCK1 domain (*right*) was developed for mSlo1 by Latorre and Brauchi [7]. The mSlo1 sequence is identical to that of hSlo1 in the RCK1 domain (see Fig. 2a). The images were prepared with MacPyMOL. (**b**) Representative G-V curves from the wild-type, D362A:D367A:E399A ("Triple") and D367A channels at pH_i=7.2 (open circles) and 6.2 (filled circles) in the absence

of Ca^{2+}. (**c**) Mean $\Delta V_{0.5}$ values in the wild-type and mutant channels caused by lowering pH_i from 7.2 to 6.2 (also see Supplementary Table 1). Error bars represent s.e.m.

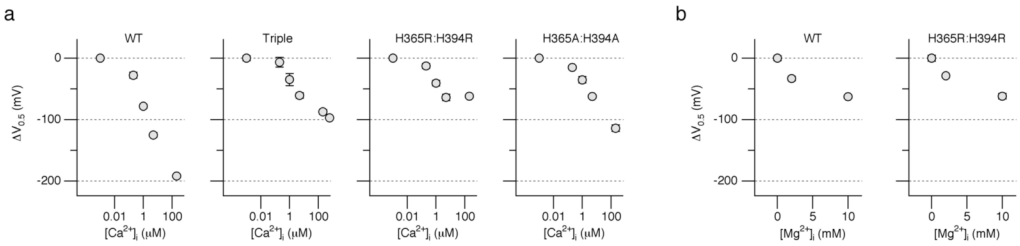

Figure 6.

Mutation of His365 and His394 disrupts the Ca^{2+}-dependent activation but fails to alter the Mg^{2+}-dependent activation. **(a)** Ca^{2+}-dependent activation measured by changes in $V_{0.5}$ in the wild-type, D362:D367:E399, H365R:H394R, and H365A:H394A channels. For each channel type, the results were normalized to the mean $V_{0.5}$ value in the virtual absence of Ca^{2+}. n = 4 to 9. (**b**) Mg^{2+}-dependent of activation measured by changes in $V_{0.5}$ in the wild-type (n = 3) and H365R:H394R channels (n = 5). Error bars represent s.e.m.